ACS MATERIALS LETTERS

www.acsmaterialsletters.org

LETTER

Synthesis and Spectroscopy of Emissive, Surface-Modified, Copper-Doped Indium Phosphide Nanocrystals

M. Elizabeth Mundy, Forrest W. Eagle, Kira E. Hughes, Daniel R. Gamelin, and Brandi M. Cossairt*

Cite This: *ACS Materials Lett.* 2020, 2, 576–581

Read Online

ACCESS | Metrics & More | Article Recommendations | Supporting Information

ABSTRACT: **Aminophosphine precursors were used to synthesize copper-doped indium phosphide nanocrystals (InP NCs) via direct doping in a slow-injection bottom-up method and postsynthetic cation exchange. By both methods, the amount of copper incorporated into the NCs could be tuned simply by varying the molar ratio during synthesis. Common postsynthetic surface modifications such as Lewis acid treatment and zinc chalcogenide shelling were performed on these samples, resulting in an enhancement of the copper-based emission from 10% to 40%. For samples with thick shells, the copper-based photoluminescence quantum yield reached over 60%, a record value for doped InP NCs. Time-resolved photoluminescence spectroscopy showed increasing carrier lifetimes after surface treatments concurrent with the disappearance of a 2 ns decay process previously attributed to surface trapping in native InP NCs, showing the broad applicability and consistent impacts of the surface treatments. In this way, we have successfully developed a route to obtain high-quality near-infrared emitters utilizing less toxic alternatives to the popular lead- and cadmium-containing materials.**

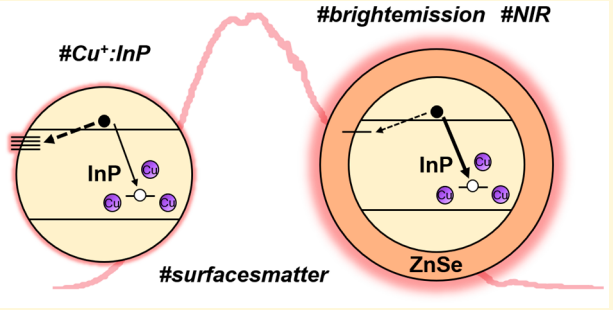

Semiconductor nanocrystals (NCs), or quantum dots, have been of great fundamental interest over the past few decades because of their solution processability and size, shape, and composition tunability. These features also make them attractive for commercial applications, including displays, lighting, photovoltaics, and biological sensing.[1−4] Copper-doped NCs, however, have captured recent attention because they exhibit Stokes-shifted emission and long photoluminescence (PL) lifetimes, properties that reflect copper's presence as a dopant in the NC lattice.[5−11] These features are particularly attractive for the design of near-infrared emitters for use in luminescent solar concentrators because of the NCs' low reabsorption and the advantageous location of the copper-based PL relative to the band gap of traditional silicon photovoltaics.[12,13] The PL in copper-doped semiconductors is attributed to localization of photogenerated valence-band holes at the Cu^{+} dopants following interband photoexcitation, formally forming Cu^{2+} in a luminescent mid-gap charge-transfer (CT) excited state.[5,14] The nuclear reorganization associated with hole localization gives the copper-based PL its characteristic broad line width, and the CT nature of the excited state contributes to its long lifetime.

Understanding charge-carrier traps is fundamental to developing the highly luminescent materials needed for a range of semiconductor technologies, including displays and photovoltaics. To be industrially relevant, NCs must have high PL quantum yields (PLQYs) and narrow PL line widths. Although cadmium selenide (CdSe) NCs with near-unity PLQYs have been obtained and are now fundamentally well-understood, synthesizing NCs of non-toxic alternatives (e.g., III−V materials) that possess similar physical properties has proven challenging.[15] Indium phosphide (InP) NCs are an exciting and commercially proven alternative to cadmium-based materials, given their inherently lower toxicity and similar optical properties.[16,17] Recent developments in InP NC syntheses have separately produced ensembles that are monodisperse and highly photo- and electroluminescent, albeit with broader PL line widths than their CdSe analogues.[18−20] Despite these advances, the underlying principles governing the increase in PLQY are still under question. Various literature reports highlight the passivation of electron or hole

Received: March 24, 2020
Accepted: April 23, 2020
Published: April 23, 2020

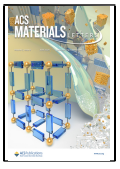

https://dx.doi.org/10.1021/acsmaterialslett.0c00112
ACS Materials Lett. 2020, 2, 576–581

traps, but the extent to which each trapping mechanism impacts the PL of InP NCs is debated.[21−23]

Using copper as an "engineered" hole trap offers a unique opportunity to examine carrier dynamics in NCs that is complementary to the study of undoped NCs. By preparing Cu^+:InP NCs, we can analyze the charge-carrier dynamics as a function of different postsynthetic surface treatments and correlate increases in PLQY with reduction in surface carrier trapping. Copper can be incorporated into the InP NCs either through a bottom-up method during synthesis or via a postsynthetic cation exchange reaction. The copper-doped cores can then be treated with Lewis acids, specifically zinc carboxylate, to increase the PLQYs using a method pioneered by our lab, while maintaining dopant incorporation.[24,25] Similar to prior literature reports, shelling the doped cores proved challenging because of copper migration from the NCs under traditional shelling conditions.[6] However, we were able to postsynthetically incorporate copper into thinly shelled InP/ZnSe NCs, inspired by an approach used for doping of CdSe/CdS NCs.[14] All of the samples were then spectroscopically probed utilizing time-resolved photoluminescence spectroscopy (TRPL) to study the recombination dynamics of the conduction-band electron and copper-localized hole.

Aminophosphines have recently generated interest as relatively environmentally benign phosphorus sources for the synthesis of a range of metal phosphide NCs.[26−31] Changing the identity of the indium and cadmium halide precursors, for example, produces size-tunable InP or Cd_3P_2 NCs.[27,30] Given the previously established reactivity of aminophosphines with transition metals, we hypothesized that this system may provide an excellent synthetic platform for generating doped InP NCs. Prior experiments in our lab showed the formation of crystalline Cu_3P platelets from $CuCl_2$ and tris(diethylamino)-phosphine (Figure S1). Although this result indicated the amenability of the system to the formation of Cu−P bonds, it also presented a challenge of preventing preferential formation of separate crystalline phases of Cu_3P and InP. This was recently seen under synthetic conditions where the presence of copper diverted significant amounts of phosphorus and allowed the formation of small InP NCs.[32] Although other reports gave no indication of the formation of Cu_3P under doping conditions, we found that this impurity persisted when the aminophosphine was injected into a solution containing both the indium and copper halides.[33,34] To circumvent this detrimental reactivity, we delayed the introduction of the copper halide by 5 min to allow the InP to nucleate. Operationally, we used a syringe pump to add a solution of copper chloride in oleylamine over 30 min. The dropwise addition also maintained a relatively low concentration of copper to prevent monomers from reaching a critical concentration and separately nucleating Cu_3P.

With our procedure established (Scheme 1), we successfully synthesized Cu^+:InP NCs. As shown in Figure 1A, the NCs synthesized with Z = 0.2 equiv of copper and $InCl_3$ exhibit the

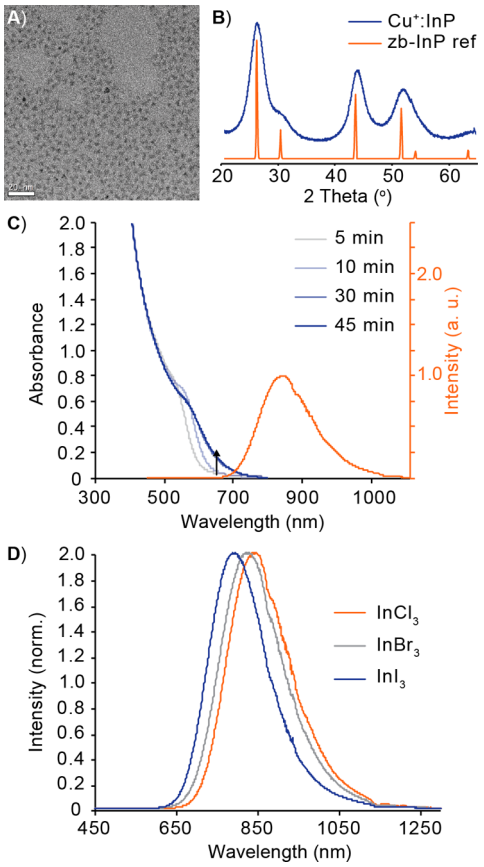

Figure 1. (A) TEM image of Cu^+:InP NCs derived from aminophosphines and $InCl_3$ showing d = 3.2 ± 0.3 nm NCs. (B) Powder X-ray diffraction pattern of the same NCs showing the only crystalline phase present to be InP (pdf 01-070-2513 ICSD). (C) UV−vis absorption spectra of reaction progress and final steady-state PL spectrum of a representative synthesis of Cu^+:InP NCs (10% PLQY). (D) Normalized steady-state PL spectra of copper-doped InP NCs synthesized with different halide precursors to tune the size of the NCs and the resulting emission energy.

characteristic tetrahedral morphology and 3.2 nm diameter associated with aminophosphine-derived InP NCs. The powder X-ray diffraction pattern (Figure 1B) is consistent with InP as the sole crystalline phase, and inductively coupled plasma optical emission spectroscopy (ICP-OES) confirmed the presence of copper in the NCs. The optical spectra strongly support copper doping (Figure 1C). Addition of copper results in the appearance of a broad red-shifted PL band with its maximum at ∼850 nm and the emergence of weak near-band-edge absorption at ∼650 nm that has been attributed to direct photoexcitation of the luminescent CT excited state.[35] Photoluminescence excitation (PLE) measurements monitoring the emission at 825 nm showed that the NIR emission arises from NC photoexcitation (Figure S2). Together, these data constitute strong support for the incorporation of copper ions into the NC lattice. These NCs exhibit high PLQYs directly out of synthesis, ranging from 8 to 25%. We found that the PLQY decreases when the reaction scale is increased, likely as a result of variations in the heating profile that lead to less uninform copper incorporation.

We investigated the tunability of this reaction with regard to NC size and amount of copper incorporated. By alteration of the amount of copper added to the reaction (Z in Scheme 1),

Scheme 1

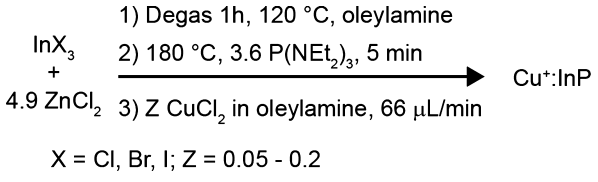

https://dx.doi.org/10.1021/acsmaterialslett.0c00112
ACS Materials Lett. 2020, 2, 576−581

the In:Cu ratio in the final products could be modestly tuned (Table S1). We found that the upper limit was an In:Cu ratio of 17:1 (5.6% replacement of In), achieved with a starting In:Cu ratio of 10:1 or 20:1 in the reaction mixture. This NC doping level corresponds to incorporation of approximately 12 copper atoms per NC. When the starting In:Cu ratio was changed to 40:1, the corresponding In:Cu ratio was decreased to 33:1, corresponding to six copper atoms per nanocrystal. Higher levels of copper incorporation could be attained by changing the copper source to the more reactive copper(II) bromide, which gave an In:Cu ratio of 4:1 while maintaining the InP crystal phase (Figure S3). However, this synthesis did not result in an increased PLQY or a dramatic shift in the PL peak position, which may suggest the presence of significant surface-bound copper.

The NC size could be tuned by following established literature procedures for aminophosphine-derived InP NCs.[27] By replacing $InCl_3$ with either $InBr_3$ or InI_3 as the indium source and utilizing our standard slow-injection procedure, we also synthesized 3.0 and 2.8 nm diameter Cu^+:InP NCs with PLQYs of 15% and 18%, respectively (Figure S4). These changes in size were accompanied by a corresponding blue shift in the copper PL peak for the smaller NCs, as can be seen in Figure 1D. Our data agree with prior reports of the tunability of both the copper PL and host NC size.[6] The size changes were accompanied by increases in the level of copper incorporation, which could be attributed to increased reactivity of the copper precursor due to partial ligand scrambling at elevated temperatures.[36,37]

An advantage of Cu^+:InP NCs as a material for photophysical studies is the localization of the hole at the copper.[5] Recent work by our group has posited that both hole trapping and electron trapping are present and account for the typically low PLQY of as-synthesized InP NCs.[21] It is hypothesized that the electron traps can be addressed by exchanging undercoordinated indium atoms at the surface via treatment with lower-valent Lewis acids, specifically for M^{2+} carboxylates.

Despite prior reports of moderate copper stability within InP NCs, excitonic PL re-emerged under traditional shelling and Lewis acid treatment conditions, signaling copper loss from a subset of NCs (Figure S5). This instability necessitated the use of a lower temperature, 100 °C compared to 200 °C, for the Lewis acid treatment with zinc stearate. At 100 °C, treatment with zinc carboxylate maintains the In:Cu ratio as determined by ICP (Table S1) while inducing an increase in PLQY from 10% to 20% for Cu^+:InP/Zn NCs with no evidence of excitonic luminescence (Figure S6). The standard aminophosphine reaction contains an excess of zinc in the nucleation pot, which has been shown to increase the monodispersity of the final NCs and likely creates a zinc-rich surface that facilitates shell growth.[29,31] However, the treatment that we perform with the zinc carboxylates clearly alters the surface chemistry and passivates defects in a way the zinc halides cannot.

Prior reports have shown that cadmium carboxylates strongly interact with the InP surface and are highly successful agents for passivating electron traps.[21,24] In this study, we found that cadmium treatment is incompatible with the doped materials; at temperatures high enough for PLQY enhancement, we observed that the dopant leaves the NCs, as confirmed by PL and ICP analysis (Figure S7). This might be due to alloying of cadmium into the surface, disrupting the lattice and accelerating copper loss.[24,38]

Shelling of previously doped NCs resulted in partial migration of copper from the lattice under a range of conditions, as reported in the literature.[27,34] Such samples demonstrated extremely high PLQYs, over 60% for the copper peak alone, but the presence of both doped and undoped NC populations in the sample limited their usefulness for spectroscopic study (Figure S8). To our knowledge, this quantum yield is the highest reported for Cu^+:InP, as prior studies reported copper-based PLQYs of up to only 40%, making this a dramatic 20% increase in PLQY.[6,9,11,33] As mentioned above, copper can be postsynthetically doped into InP NC cores and has been previously shown to incorporate postsynthetically into II–VI NCs with thin shells.[6,14] Using this established precedent, we explored copper incorporation in thinly (~1 monolayer) ZnSe-shelled InP NCs via cation exchange.[6,14] A copper chloride solution was added after shelling, and within 2 h the excitonic PL disappeared and the characteristic copper PL dominated the spectrum, with a PLQY of 40% (Figure 2). An initial 10:1 In:Cu molar ratio

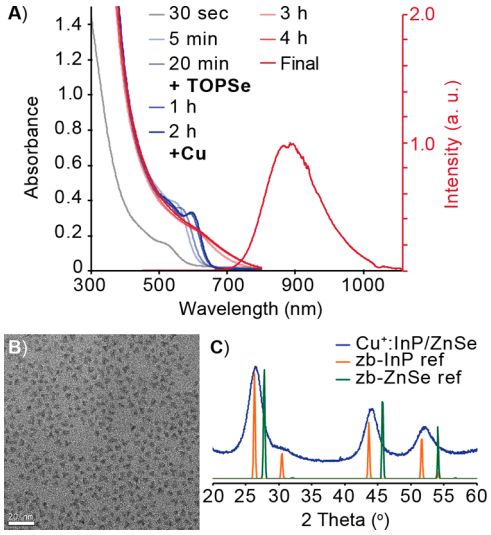

Figure 2. (A) UV–vis absorption spectra of reaction progress and final steady-state PL spectrum of a representative synthesis of Cu^+:InP/ZnSe NCs (40% PLQY). (B) TEM of Cu^+:InP/ZnSe NCs showing $d = 4.2 \pm 0.4$ nm. (C) Powder X-ray diffraction pattern of the same NCs showing the crystalline phase present to be primarily InP (pdf 01-070-2513 ICSD) with slight shifts toward ZnSe (pdf 01-071-5977 ICSD).

produced NCs with a final In:Cu ratio of 14:1, similar to the upper limit seen in the bottom-up synthesis. Thick-shelled InP NCs were also doped via the same method, but the time needed for copper diffusion exceeded 12 h (Figure S9) with no comparative increase in PLQY relative to the thinly shelled materials. This may be due to distribution of copper throughout both the nanocrystal core and shell in these samples.

Previous work showed that native carboxylate-ligated InP NCs exhibit electron trapping at undercoordinated indium sites within ~10 ns and subnanosecond hole trapping.[21,22] These trap states can be passivated by various surface treatments; in the case of our aminophosphine NCs, a zinc carboxylate treatment passivates electron traps by exchanging with either undercoordinated indium ions on the NC surface or datively bound Lewis bases like primary amine, while zinc

https://dx.doi.org/10.1021/acsmaterialslett.0c00112
ACS Materials Lett. 2020, 2, 576–581

chalcogenide shelling can passivate both electron and hole traps.[21]

As discussed above, upon introduction of Cu^+ into the InP NC lattice, the PLQY increases from ∼1% to 10%, suggesting that the Cu^+ competes effectively with native surface traps for capture of the photogenerated hole. However, it is likely that a PLQY of only 10% still indicates the presence of significant carrier trapping at the NC surface. Therefore, the aforementioned surface treatments should help remove potential trap sites and increase the sample PLQY. We used TRPL spectroscopy to study recombination of the photogenerated delocalized conduction-band electron with the copper-localized hole as a function of these NC surface treatments.

Figure 3 shows PL decay curves measured for Cu^+:InP, Cu^+:InP/Zn, and Cu^+:InP/ZnSe NCs, plotted on a 1 μs window. Fitting the PL decay of the untreated Cu^+:InP NCs to a biexponential function gives a weighted PL lifetime of 272 ns (see the Supporting Information for fitting parameters). This result aligns well with previous reports of long luminescence lifetimes in copper-doped NCs, but the decay lifetime here is slightly shorter than the ∼500 ns lifetime reported for Cu^+:InP/ZnS/InP/ZnS NCs.[39] This discrepancy could be due to a difference in the physical structures of the two materials, or it could indicate that our system still has competing carrier trapping pathways.[17] The PL decay of the Cu^+:InP/Zn NC sample is nearly identical (Figure 3), with a weighted lifetime of 313 ns. The Cu^+:InP/ZnSe NC sample, however, has a much longer lifetime of 383 ns, indicating the efficiency with which even a thin layer of ZnSe can eliminate surface traps.

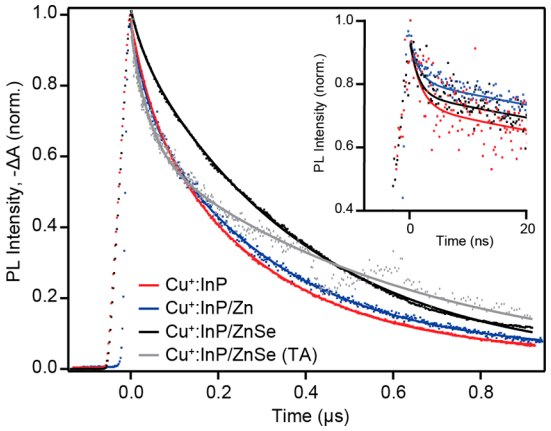

Figure 3. Normalized PL decay dynamics of the copper PL for Cu^+:InP NCs (red), Cu^+:InP/Zn NCs (blue), and Cu^+:InP/ZnSe NCs (black). The inset shows the first 20 ns of data collected in a 100 ns window (Figure S10). In addition, normalized TA ($-\Delta A$) data are shown for Cu^+:InP/ZnSe NCs (gray). All of the data were collected at room temperature on NCs suspended in dry toluene. The untreated Cu^+:InP NCs (red) show the fastest decay and have the lowest PLQY of 10%, followed by the Cu^+:InP/Zn NCs (blue, PLQY of 20%), and finally, the shelled Cu^+:InP/ZnSe NCs (black) show the longest lifetime and highest PLQY of 40%. PL data were acquired using an excitation wavelength of 365 nm, and PL decay curves were obtained by integrating between 780 and 880 nm. TA data were acquired using a 365 nm pump pulse followed by a continuum white-light probe pulse. The dynamics was obtained by integration of the TA bleach between 654 and 714 nm.

Despite similarities in the decay dynamics of the Cu^+:InP and Cu^+:InP/Zn NC samples, the PLQY of the Cu^+:InP/Zn NCs is 20%, double that of the Cu^+:InP NCs. Therefore, we also examined the PL decay dynamics on a 100 ns time scale (Figure 3 inset and Figure S10) to attempt to observe faster processes. The Cu^+:InP and Cu^+:InP/Zn NCs appear to have very similar decay dynamics on this time scale as well, but the Cu^+:InP NCs decay almost twice as much as the Cu^+:InP/Zn NCs in the first ∼2 ns. This result shows that the zinc carboxylate surface treatment doubles the PLQY by eliminating trapping processes that occur on this time scale. The Cu^+:InP/ZnSe NCs also exhibit less ∼2 ns decay than the Cu^+:InP NCs, and their slower decay on the 1 μs time scale accounts for their higher PLQY compared with the Cu^+:InP/Zn NCs. Moreover, examination of the excitonic bleach recovery dynamics of Cu^+:InP/ZnSe using transient absorption (TA) spectroscopy shows significant deviation from the corresponding TRPL data at early times (Figures S14−S16). The observation of faster dynamics in the TA spectra provides strong support for hole localization at copper prior to other trapping processes and suggests that any differences in the decay dynamics we observe among surface-treated samples are due to differences in electron trapping. Since the TRPL specifically monitors the copper luminescence, the hole must be localized at copper for that signal to be observed. The presence of a faster component in the TA dynamics, however, indicates that trapping contributes to faster decay of the conduction-band electron (and hence the TA signal), consistent with the 40−45% PLQY. While fast hole trapping due to nonluminescent surface-bound copper ions has been previously implicated in Cu^+:InP,[40] we find this to be an unlikely explanation in the present system because of the observed trends in the fast-time TRPL data and the comparison with the TA dynamics.

In summary, we have developed a synthetic route to access highly luminescent copper-doped InP NCs from aminophosphine and metal halide precursors. The copper content can be tuned by altering the initial molar ratio or through postsynthetic cation exchange, and the copper PL energy can be shifted by changing the indium precursor, which controls the size of the final NCs. Upon surface modification, either by Lewis acid treatment with zinc carboxylate or by growth of a thin ZnSe shell, the PLQY increases. This PLQY increase is correlated with the decrease of an ∼2 ns PL decay component and, in the case of the Cu^+:InP/ZnSe NCs, also with slower PL decay over the subsequent hundreds of nanoseconds. This work demonstrates that similar trapping processes occur in doped and undoped InP NCs and that surface treatments first developed for undoped InP NCs are effective in eliminating competing trap pathways in doped InP NCs as well. We are able to synthesize highly luminescent Cu^+:InP NCs and demonstrate the applicability of postsynthetic surface modification for doped NC emitters.

■ ASSOCIATED CONTENT

Supporting Information

The Supporting Information is available free of charge at https://pubs.acs.org/doi/10.1021/acsmaterialslett.0c00112.

Additional data, data analysis, and experimental details (PDF)

https://dx.doi.org/10.1021/acsmaterialslett.0c00112
ACS Materials Lett. 2020, 2, 576−581

AUTHOR INFORMATION

Corresponding Author

Brandi M. Cossairt − *Department of Chemistry, University of Washington, Seattle, Washington 98195-1700, United States;* orcid.org/0000-0002-9891-3259; Email: cossairt@uw.edu

Authors

M. Elizabeth Mundy − *Department of Chemistry, University of Washington, Seattle, Washington 98195-1700, United States*

Forrest W. Eagle − *Department of Chemistry, University of Washington, Seattle, Washington 98195-1700, United States*

Kira E. Hughes − *Department of Chemistry, University of Washington, Seattle, Washington 98195-1700, United States;* orcid.org/0000-0001-6454-8700

Daniel R. Gamelin − *Department of Chemistry, University of Washington, Seattle, Washington 98195-1700, United States;* orcid.org/0000-0003-2888-9916

Complete contact information is available at: https://pubs.acs.org/10.1021/acsmaterialslett.0c00112

Author Contributions

The manuscript was written through contributions of all authors.

Notes

The authors declare no competing financial interest.

ACKNOWLEDGMENTS

This research was supported by the National Science Foundation (NSF) through the UW Molecular Engineering Materials Center, a Materials Research Science and Engineering Center (DMR-1719797 to B.M.C. and D.R.G.). Part of this work was conducted at the Molecular Analysis Facility, a National Nanotechnology Coordinated Infrastructure Site at the University of Washington that is supported in part by the National Science Foundation (Grant NNCI-1542101), the University of Washington, the Molecular Engineering & Sciences Institute, and the Clean Energy Institute. We also gratefully acknowledge Reviewer 3 for insightful comments that contributed meaningfully to the revision of this Letter.

REFERENCES

(1) Talapin, D. V.; Steckel, J. Quantum Dot Light-Emitting Devices. *MRS Bull.* **2013**, *38*, 685−691.

(2) Talapin, D. V.; Lee, J.-S.; Kovalenko, M. V.; Shevchenko, E. V. Prospects of Colloidal Nanocrystals for Electronic and Optoelectronic Applications. *Chem. Rev.* **2010**, *110*, 389−458.

(3) Kramer, I. J.; Sargent, E. H. Colloidal Quantum Dot Photovoltaics: A Path Forward. *ACS Nano* **2011**, *5*, 8506−8514.

(4) Medintz, I.; Uyeda, H.; Goldman, E.; Mattoussi, H. Quantum Dot Bioconjugates for Imaging, Labelling and Sensing. *Nat. Mater.* **2005**, *4*, 435−446.

(5) Knowles, K. E.; Hartstein, K. H.; Kilburn, T. B.; Marchioro, A.; Nelson, H. D.; Whitham, P. J.; Gamelin, D. R. Luminescent Colloidal Semiconductor Nanocrystals Containing Copper: Synthesis, Photophysics, and Applications. *Chem. Rev.* **2016**, *116*, 10820−10851.

(6) Xie, R.; Peng, X. Synthesis of Cu-Doped InP Nanocrystals (d-Dots) with ZnSe Diffusion Barrier as Efficient and Color-Tunable NIR Emitters. *J. Am. Chem. Soc.* **2009**, *131*, 10645−10651.

(7) Srivastava, B. B.; Jana, S.; Pradhan, N. Doping Cu in Semiconductor Nanocrystals: Some Old and Some New Physical Insights. *J. Am. Chem. Soc.* **2011**, *133*, 1007−1015.

(8) Grandhi, G. K.; Viswanatha, R. Tunable Infrared Phosphors Using Cu Doping in Semiconductor Nanocrystals: Surface Electronic Structure Evaluation. *J. Phys. Chem. Lett.* **2013**, *4*, 409−415.

(9) Knowles, K. E.; Nelson, H. D.; Kilburn, T. B.; Gamelin, D. R. Singlet−Triplet Splittings in the Luminescent Excited States of Colloidal Cu+:CdSe, Cu+:InP, and CuInS2 Nanocrystals: Charge-Transfer Configurations and Self-Trapped Excitons. *J. Am. Chem. Soc.* **2015**, *137*, 13138−13147.

(10) Cooper, J. K.; Gul, S.; Lindley, S. A.; Yano, J.; Zhang, J. Z. Tunable Photoluminescent Core/Shell Cu+-Doped ZnSe/ZnS Quantum Dots Codoped with Al3+, Ga3+, or In3+. *ACS Appl. Mater. Interfaces* **2015**, *7*, 10055−10066.

(11) Hassan, A.; Zhang, X.; Liu, X.; Rowland, C. E.; Jawaid, A. M.; Chattopadhyay, S.; Gulec, A.; Shamirian, A.; Zuo, X.; Klie, R. F.; Schaller, R. D.; Snee, P. T. Charge Carriers Modulate the Bonding of Semiconductor Nanoparticle Dopants As Revealed by Time-Resolved X-ray Spectroscopy. *ACS Nano* **2017**, *11*, 10070−10076.

(12) Sharma, M.; Gungor, K.; Yeltik, A.; Olutas, M.; Guzelturk, B.; Kelestemur, Y.; Erdem, T.; Delikanli, S.; McBride, J. R.; Demir, H. V. Near-Unity Emitting Copper-Doped Colloidal Semiconductor Quantum Wells for Luminescent Solar Concentrators. *Adv. Mater.* **2017**, *29*, 1700821.

(13) Bradshaw, L. R.; Knowles, K. E.; McDowall, S.; Gamelin, D. R. Nanocrystals for Luminescent Solar Concentrators. *Nano Lett.* **2015**, *15*, 1315−1323.

(14) Hughes, K. E.; Hartstein, K. H.; Gamelin, D. R. Photodoping and Transient Spectroscopies of Copper-Doped CdSe/CdS Nanocrystals. *ACS Nano* **2018**, *12*, 718−728.

(15) Hanifi, D. A.; Bronstein, N. D.; Koscher, B. A.; Nett, Z.; Swabeck, J. K.; Takano, K.; Schwartzberg, A. M.; Maserati, L.; Vandewal, K.; van de Burgt, Y.; Salleo, A.; Alivisatos, A. P. Redefining Near-Unity Luminescence in Quantum Dots with Photothermal Threshold Quantum Yield. *Science* **2019**, *363*, 1199.

(16) Tarantini, A.; Wegner, K. D.; Dussert, F.; Sarret, G.; Beal, D.; Mattera, L.; Lincheneau, C.; Proux, O.; Truffier-Boutry, D.; Moriscot, C.; Gallet, B.; Jouneau, P.-H.; Reiss, P.; Carrière, M. Physicochemical Alterations and Toxicity of InP Alloyed Quantum Dots Aged in Environmental Conditions: A Safer by Design Evaluation. *NanoImpact* **2019**, *14*, 100168.

(17) Wegner, K. D.; Dussert, F.; Truffier-Boutry, D.; Benayad, A.; Beal, D.; Mattera, L.; Ling, W. L.; Carrière, M.; Reiss, P. Influence of the Core/Shell Structure of Indium Phosphide Based Quantum Dots on Their Photostability and Cytotoxicity. *Front. Chem.* **2019**, *7*, 466.

(18) Won, Y.-H.; Cho, O.; Kim, T.; Chung, D.-Y.; Kim, T.; Chung, H.; Jang, H.; Lee, J.; Kim, D.; Jang, E. Highly Efficient and Stable InP/ZnSe/ZnS Quantum Dot Light-Emitting Diodes. *Nature* **2019**, *575*, 634−638.

(19) Kim, Y.; Ham, S.; Jang, H.; Min, J. H.; Chung, H.; Lee, J.; Kim, D.; Jang, E. Bright and Uniform Green Light Emitting InP/ZnSe/ZnS Quantum Dots for Wide Color Gamut Displays. *ACS Appl. Nano Mater.* **2019**, *2*, 1496−1504.

(20) Ramasamy, P.; Ko, K.-J.; Kang, J.-W.; Lee, J.-S. Two-Step "Seed-Mediated" Synthetic Approach to Colloidal Indium Phosphide Quantum Dots with High-Purity Photo- and Electroluminescence. *Chem. Mater.* **2018**, *30*, 3643−3647.

(21) Hughes, K. E.; Stein, J. L.; Friedfeld, M. R.; Cossairt, B. M.; Gamelin, D. R. Effects of Surface Chemistry on the Photophysics of Colloidal InP Nanocrystals. *ACS Nano* **2019**, *13*, 14198−14207.

(22) Janke, E. M.; Williams, N. E.; She, C.; Zherebetskyy, D.; Hudson, M. H.; Wang, L.; Gosztola, D. J.; Schaller, R. D.; Lee, B.; Sun, C.; Engel, G. S.; Talapin, D. V. Origin of Broad Emission Spectra in InP Quantum Dots: Contributions from Structural and Electronic Disorder. *J. Am. Chem. Soc.* **2018**, *140*, 15791−15803.

(23) Richter, A. F.; Binder, M.; Bohn, B. J.; Grumbach, N.; Neyshtadt, S.; Urban, A. S.; Feldmann, J. Fast Electron and Slow Hole Relaxation in InP-Based Colloidal Quantum Dots. *ACS Nano* **2019**, *13*, 14408−14415.

(24) Stein, J. L.; Mader, E. A.; Cossairt, B. M. Luminescent InP Quantum Dots with Tunable Emission by Post-Synthetic Modification with Lewis Acids. *J. Phys. Chem. Lett.* **2016**, *7*, 1315−1320.

(25) Kirkwood, N.; Monchen, J. O. V.; Crisp, R. W.; Grimaldi, G.; Bergstein, H. A. C.; du Fossé, I.; van der Stam, W.; Infante, I.;

Houtepen, A. J. Finding and Fixing Traps in II−VI and III−V Colloidal Quantum Dots: The Importance of Z-Type Ligand Passivation. *J. Am. Chem. Soc.* **2018**, *140*, 15712−15723.
(26) Tessier, M. D.; De Nolf, K.; Dupont, D.; Sinnaeve, D.; De Roo, J.; Hens, Z. Aminophosphines: A Double Role in the Synthesis of Colloidal Indium Phosphide Quantum Dots. *J. Am. Chem. Soc.* **2016**, *138*, 5923−5929.
(27) Tessier, M. D.; Dupont, D.; De Nolf, K.; De Roo, J.; Hens, Z. Economic and Size-Tunable Synthesis of InP/ZnE (E = S, Se) Colloidal Quantum Dots. *Chem. Mater.* **2015**, *27*, 4893−4898.
(28) Buffard, A.; Dreyfuss, S.; Nadal, B.; Heuclin, H.; Xu, X.; Patriarche, G.; Mézailles, N.; Dubertret, B. Mechanistic Insight and Optimization of InP Nanocrystals Synthesized with Aminophosphines. *Chem. Mater.* **2016**, *28*, 5925−5934.
(29) Laufersky, G.; Bradley, S.; Frécaut, E.; Lein, M.; Nann, T. Unraveling Aminophosphine Redox Mechanisms for Glovebox-Free InP Quantum Dot Syntheses. *Nanoscale* **2018**, *10*, 8752−8762.
(30) Mundy, M. E.; Ung, D.; Lai, N. L.; Jahrman, E. P.; Seidler, G. T.; Cossairt, B. M. Aminophosphines as Versatile Precursors for the Synthesis of Metal Phosphide Nanocrystals. *Chem. Mater.* **2018**, *30*, 5373−5379.
(31) Song, W.-S.; Lee, H.-S.; Lee, J. C.; Jang, D. S.; Choi, Y.; Choi, M.; Yang, H. Amine-Derived Synthetic Approach to Color-Tunable InP/ZnS Quantum Dots with High Fluorescent Qualities. *J. Nanopart. Res.* **2013**, *15*, 1750.
(32) Huang, F.; Bi, C.; Guo, R.; Zheng, C.; Ning, J.; Tian, J. Synthesis of Colloidal Blue-Emitting InP/ZnS Core/Shell Quantum Dots with the Assistance of Copper Cations. *J. Phys. Chem. Lett.* **2019**, *10*, 6720−6726.
(33) Mei, S.; Wei, X.; Yang, D.; Su, D.; Yang, W.; Zhang, G.; Hu, Z.; Yang, B.; Dai, H.; Xie, F.; Zhang, W.; Guo, R. Color-Tunable Optical Properties of Cadmium-Free Transition Metal Ions Doped InP/ZnS Quantum Dots. *J. Lumin.* **2019**, *212*, 264−270.
(34) Wei, X.; Mei, S.; Zhang, G.; Su, D.; Xie, F.; Zhang, W.; Guo, R. Enhanced Tunable Dual Emission of Cu:InP/ZnS Quantum Dots Enabled by Introducing Ag Ions. *Appl. Surf. Sci.* **2019**, *493*, 605−612.
(35) Yang, L.; Knowles, K. E.; Gopalan, A.; Hughes, K. E.; James, M. C.; Gamelin, D. R. One-Pot Synthesis of Monodisperse Colloidal Copper-Doped CdSe Nanocrystals Mediated by Ligand−Copper Interactions. *Chem. Mater.* **2016**, *28*, 7375−7384.
(36) Ruberu, T. P. A.; Albright, H. R.; Callis, B.; Ward, B.; Cisneros, J.; Fan, H.-J.; Vela, J. Molecular Control of the Nanoscale: Effect of Phosphine−Chalcogenide Reactivity on CdS−CdSe Nanocrystal Composition and Morphology. *ACS Nano* **2012**, *6*, 5348−5359.
(37) Hunt, C. T.; Balch, A. L. Scrambling of Halide Ligands between Palladium(II) and between Palladium(I) Complexes of Bis-(Diphenylphosphino)Methane. Observation of Unusual Temperature-Dependent Phosphorus-31 NMR Chemical Shifts. *Inorg. Chem.* **1982**, *21*, 1641−1644.
(38) Stein, J. L.; Steimle, M. I.; Terban, M. W.; Petrone, A.; Billinge, S. J. L.; Li, X.; Cossairt, B. M. Cation Exchange Induced Transformation of InP Magic-Sized Clusters. *Chem. Mater.* **2017**, *29*, 7984−7992.
(39) Zhang, Z.; Liu, D.; Li, D.; Huang, K.; Zhang, Y.; Shi, Z.; Xie, R.; Han, M.-Y.; Wang, Y.; Yang, W. Dual Emissive Cu:InP/ZnS/InP/ZnS Nanocrystals: Single-Source "Greener" Emitters with Flexibly Tunable Emission from Visible to Near-Infrared and Their Application in White Light-Emitting Diodes. *Chem. Mater.* **2015**, *27*, 1405−1411.
(40) Hassan, A.; Zhang, X.; Liu, C.; Snee, P. T. Electronic Structure and Dynamics of Copper-Doped Indium Phosphide Nanocrystals Studied with Time-Resolved X-ray Absorption and Large-Scale DFT Calculations. *J. Phys. Chem. C* **2018**, *122*, 11145−11151.

https://dx.doi.org/10.1021/acsmaterialslett.0c00112
ACS Materials Lett. 2020, 2, 576−581